J Med Sci 2023;43 (6):269-275 DOI: 10.4103/jmedsci.jmedsci 244 22

ORIGINAL ARTICLE



A Simple Method for Calculating Acetabular Posterior Wall Fracture Fragment Percentages on Three-Dimensional Computed Tomography Scan Reconstruction Images

Chun-Liang Hsu¹, Jia-Lin Wu^{2,3}, Yao-Tung Tsai¹, Chun-Chi Hung¹, Yuan-Ta Li¹, Tsu-Te Yeh¹

¹Department of Orthopaedic Surgery, Tri-Service General Hospital, National Defense Medical Center, ²Department of Orthopedics, Taipei Medical University, ³Department of Orthopedics, Taipei Medical University Hospital, Taipei, Taiwan

Background: Hip joint congruency and stability in fractures are affected by posterior wall fragment size and percentage compared with the normal side. Computed tomography (CT) scan is a useful tool to precisely evaluate the morphologic features of acetabular fractures. Aim: The aim of this study was to establish an accurate and reliable method of measuring acetabular posterior wall fracture fragment percentages on three-dimensional (3D) CT scan reconstruction images. Methods: CT scans of eight patients with acetabular posterior wall fractures were reviewed by five orthopedic surgeons. Posterior wall fracture fragment percentages were measured using three methods: (1) linear measurement percentages on axial CT images, (2) linear measurement percentages on 3D reconstruction images, and (3) acetabular posterior surface area measurements using computer software (gold standard). Analysis of variance testing was used to compare these methods. Dunn's multiple comparison test was used to compare the accuracy of the axial CT scan and 3D reconstruction methods to the gold standard method. Results: There were no significant differences between two of the eight patients (25%) in fracture fragment percentage measurements using all methods. Dunn's multiple comparison test showed that the axial CT scan method measurement was significantly different from the gold standard measurement in four of the eight patients (50%), three of whom sustained more than an 80% fracture. However, there was no significant difference between the 3D reconstruction and gold standard methods in all study patients. Inter- and intra-observer reliabilities were excellent for all three methods. Conclusion: The 3D reconstruction image method is reliable and accurate for measuring acetabular posterior wall fracture fragment percentages.

Key words: Three-dimensional reconstruction, acetabular posterior wall fracture fragment percentage, computed tomography, pelvic fracture, personalized

INTRODUCTION

The acetabulum comprises the anterior column, posterior column, anterior wall, and posterior wall. Posterior wall fracture is one of the most frequent hip fracture patterns. In hip fracture, joint congruency and stability are affected by the posterior wall fragment size and percentage relative to the contralateral side. The posterior wall fragment is a critical factor affecting the treatment and clinical outcomes, particularly in patients with acetabular fractures.^{1,2} Clinically, the morphologic features of acetabular fractures can be determined precisely using computed tomography (CT) imaging.³

Received: November 08, 2022; Revised: November 22, 2022; Accepted: November 24, 2022; Published: February 08, 2023 Corresponding Author: Dr. Tsu-Te Yeh, Department of Orthopaedic Surgery, Tri-Service General Hospital, National Defense Medical Center, No. 325, Sec. 2, Chenggong Rd., Neihu Dist., Taipei 114, Taiwan. Tel: +886-2-87923311 ext 16909; Fax: +886-2-87927186. E-mail: tsutey@gmail.com

Several methods have been developed to determine the stability of posterior wall acetabular fractures, including the acetabular arc angle⁴⁻⁶ and the fracture percentage. However, an accurate and precise method of measuring the posterior wall fragment percentage has not been identified. Currently, the most widely used method involves measuring the posterior wall fragment percentage on axial view CT scan images. Reagan *et al.* reported the use of CT to predict hip instability in acetabular posterior wall fractures that exceeded 50%.

This is an open access journal, and articles are distributed under the terms of the Creative Commons Attribution-NonCommercial-ShareAlike 4.0 License, which allows others to remix, tweak, and build upon the work non-commercially, as long as appropriate credit is given and the new creations are licensed under the identical terms.

For reprints contact: WKHLRPMedknow_reprints@wolterskluwer.com

How to cite this article: Hsu CL, Wu JL, Tsai YT, Hung CC, Li YT, Yeh TT. A simple method for calculating acetabular posterior wall fracture fragment percentages on three-dimensional computed tomography scan reconstruction images. J Med Sci 2023;43:269-75.

However, in fractures <50%, hip stability should be tested by examination under anesthesia.⁷ Moed *et al.* identified some pitfalls that led to potential technical difficulties with CT measurements.⁸ However, the true posterior wall fragment percentage should be calculated using surface area ratios on three-dimensional (3D) images instead of the linear distance ratio on two-dimensional images.

The first aim of this study was to establish a gold standard method for calculating the true acetabular posterior and fracture fragment surface areas using 3D reconstruction images. The second aim was to establish a new and simple method for calculating the posterior wall fracture fragment percentage on a 3D reconstruction image. We hypothesized that this new method would be more accurate than the conventional axial CT scan method.

MATERIALS AND METHODS

Ethical approval

This study proposal was approved by the Institutional Review Board (IRB) of the Tri-Service General Hospital (2-106-05-092) (December 22, 2018).

Settings and design

This retrospective study was approved by the IRB of the Tri-Service General Hospital (IRB approval number: 2-106-05-092). The informed consents were obtained from all participants. The data of eight patients who underwent open reduction and internal fixation for acetabular posterior wall fractures from June 2014 to June 2017 were obtained from the operative database of the senior author. The sole inclusion criterion was a history of surgery for a simple acetabular posterior wall fracture. Patients were excluded if the acetabular posterior wall fracture had a concomitant posterior column or anterior column involvement. All patients underwent preoperative CT scans.

The five orthopedic surgeons selected to review the CT scans included a senior attending physician, three junior attending physicians, and a senior resident physician. The percentages of the posterior wall fracture fragments were measured using each of the following three methods: (1) measurement from the axial CT scan image, 8 (2) measurement from the 3D reconstruction image, and (3) measurement of the real surface area using software-generated 3D reconstruction images (gold standard control).

In method 1, Digital Imaging and Communication in Medicine files of CT data were converted and imported into a medical imaging processing software package (Materialise Mimics, version 21; Materialise NV, Leuven, Belgium). The width of the posterior wall fracture fragment (X) was determined from the medial extent of the quadrilateral plate

at the level of the greatest posterior wall fracture fragment. The intact matched contralateral acetabular depth (Y) was measured from the medial extent of the quadrilateral plate at a level comparable to that used to measure the fracture fragment. The percentage of the fracture fragment was calculated as X divided by Y and was multiplied by 100 (%) to yield a percentage [Figure 1].

In method 2, measurements were obtained from 3D-model images processed using Materialise Mimics software. Using the posterior view of the 3D reconstruction image, the appropriate length was measured from a line (X') starting from the point of the smallest remaining intact posterior wall and extending to a point on the posterior column, which was perpendicular to the line of the posterior column. The intact contralateral acetabular length was measured from a line (Y') starting from the median point of the acetabular rim and extending to a point on the posterior column, which was perpendicular to the posterior column. The percentage of the fracture fragment was calculated as Y'-X' divided by Y' and multiplied by 100 (%) to yield a percentage [Figure 2].

In method 3, the surface area of the posterior acetabulum was measured using Materialise Mimics and Materialise 3-matic software (version 13) according to the following steps: (1) Four points (point 1: top of the acetabular rim; point 2: top of the posterior column; point 3: inferior portion of the ischial spine; and point 4: bottom of the acetabular rim) were determined as the four corners [Figure 3a]. (2) The quadrilateral plate plane was determined [Figure 3b]. (3) Cutting plane 1 was set from point 1 to point 2, which was perpendicular to the quadrilateral plate plane. Cutting plane 2 was set from point 3 to point 4, which was perpendicular to the quadrilateral plate plane [Figure 3c]. (4) The gold standard posterior acetabular

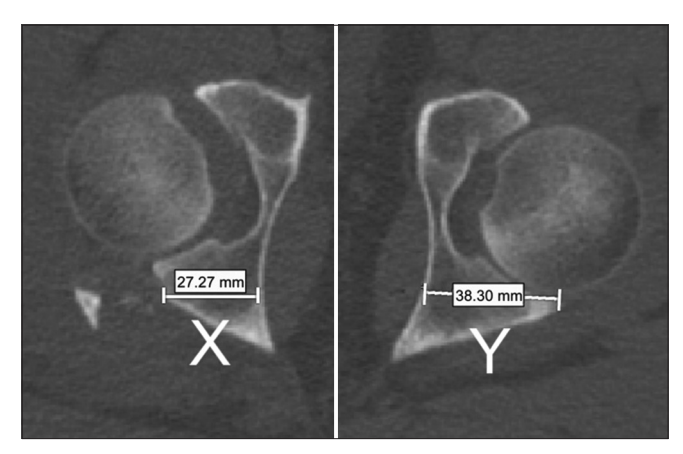


Figure 1: Representative clinical example (patient 6) of the axial computed tomography scan measurement method. The remaining intact posterior wall measurement is 22.27 mm (X), and the contralateral intact posterior wall measurement is $38.30 \, \text{mm}$ (Y). The percentage of posterior wall involvement is calculated as: $([Y-X]/Y) \times 100\% = ([38.30-27.27]/38.30) \times 100\% = 29\%$

surface area was defined as the area surrounded by cutting plane 1, cutting plane 2, the quadrilateral plate plane, and the acetabular posterior rim [Figure 3d]. The surface area (Y") was measured by marking the area with a brush tool in the 3-matic software program [Figure 3e]. The posterior wall fracture fragment surface area (X") was measured by marking the area with a brush tool in 3-matic software. The percentage of the fracture fragment was calculated as X" divided by Y" and multiplied by 100 (%) to yield a percentage [Figure 3f].

Statistical analysis used

Each orthopedist reviewed images of the eight patients and applied each of the measurement methods (Round 1). The images were again reviewed after a minimum interval of 1 month to assess the intra-observer reliability (Round 2). The measurements calculated using each of the three methods were compared using a Kruskal–Wallis one-way analysis of variance. A follow-up pairwise comparison was conducted using Dunn's multiple comparison test. Inter- and intra-observer reliabilities were evaluated using the intraclass correlation coefficient (ICC). P < 0.05 indicated statistical significance. The ICCs were interpreted as follows: <0.5, poor; 0.5–0.75, moderate; 0.75–0.9, good; and >0.9, excellent. 9.10 All statistical analyses were performed using SPSS 22.0 software (IBM Corp., Armonk, NY, USA)

RESULTS

The demographic data of the eight patients are shown in Table 1. The measured fracture fragment percentages obtained using each of the three methods did not significantly different

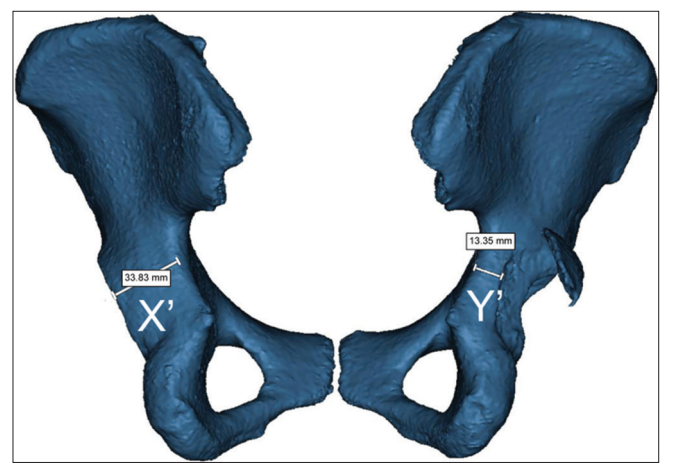


Figure 2: Representative clinical example (patient 5) of the three-dimensional reconstruction image measurement method. The remaining intact posterior wall measurement is 13.35 mm (X'), and the contralateral intact posterior wall measurement is 33.83 mm (Y'). The percentage of posterior wall involvement is calculated as: $([Y'-X']/Y') \times 100\% = ([33.83 - 13.35]/33.83) \times 100\% = 61\%$

in two of eight patients (patient 2, P=0.961 and patient 7, P=0.055). Dunn's multiple comparison test revealed that in four of eight patients (50%, patients 3, 4, 6, and 8), the axial CT scan measurement method results were significantly different from the gold standard measurement method results. In contrast, no significant differences were observed between the 3D reconstruction measurement method results and the gold standard measurement method results in any of the study patients [Table 2].

Excellent inter-observer reliability was observed among all

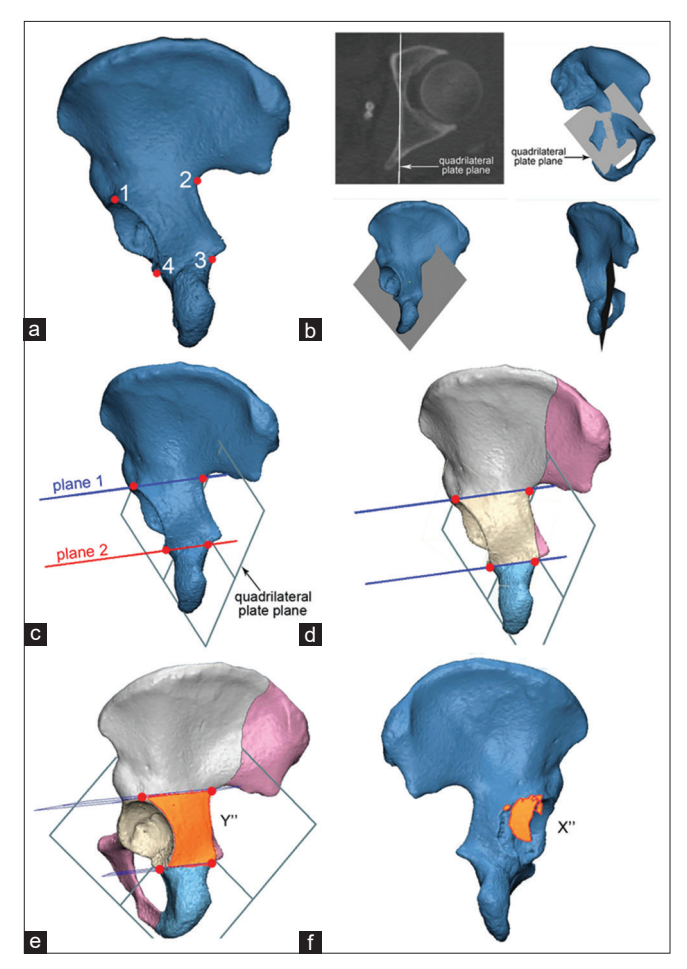


Figure 3: Representative clinical example (patient 1) of the gold-standard measurement method. (a) Identification of four points as the four corners (point 1: top of the acetabular rim; point 2: top of the posterior column; point 3: inferior portion of the ischial spine; point 4: bottom of the acetabular rim), (b) Determination of the quadrilateral plate plane, (c) Placement of cutting plane 1 from point 1 to point 2, perpendicular to the quadrilateral plate plane, and of plane 2 from point 3 to point 4, perpendicular to the quadrilateral plate plane, (d) Definition of the acetabular region (ivory) by the region cut by the quadrilateral plate plane, cutting plane 1 and cutting plane 2, (e) Calculation of the gold-standard posterior acetabular surface area (Y"=2340.5856 mm²), shown in orange, by marking the area using the brush tool in the 3-matic software program, (f) Calculation of the fracture fragment area (X"=737.8588 mm²), shown in orange, by marking the area using the brush tool in the 3-matic software program. The percentage of posterior wall involvement is calculated as: (X"/Y") × 100% = (737.8588/2340.5856) × 100% = 32%.

Table 1: Demographics of patients included in the retrospective analysis

Variable	Data
Number of patients	8
Age (years), mean (range)	38.5 (20-66)
Sex $(n)^a$	
Men	7
Women	1
Injured side (n)	
Right	6
Left	2

^an=Number of patients

the raters and for all three methods (ICC: 0.950 for the axial CT scan method, 0.949 for the 3D reconstruction method, and 0.995 for the gold-standard surface area method). The excellent level of intra-observer reliability also demonstrated the reproducibility of the three methods (ICC: 0.960 for the axial CT scan method, 0.984 for the 3D reconstruction method, and 0.993 for the gold standard surface area method). All physicians achieved excellent intra-observer reliability for each of the three methods [Table 3].

DISCUSSION

Measurement of the fragment proportions or quantitative assessment of the acetabular bone defects is important in the preoperative evaluation of acetabular posterior wall fractures, 11,12 as the posterior wall fracture fragment percentage is a predictor of hip joint instability. As noted, three methods are used to measure the percentage of posterior wall fracture fragments using axial CT scan images. This study identified a technique for measuring the standard posterior acetabular and fracture fragment surface areas using 3D reconstruction images. We also developed a new method for calculating the posterior wall fracture fragment percentage from these 3D reconstruction images. Notably, our new method achieved excellent inter-and intra-observer reliability.

Previously, Harnroongroj *et al.* measured the length of the posterior acetabular arc by dividing the injured side by the uninjured side.⁴ Reagan *et al.* calculated the ratio of fracture fragment to reference the level of the fovea by drawing a line from the medial to the lateral depth at this level.⁷ Moed *et al.* suggested using the level of the largest-sized posterior wall fracture fragment relative to the same level on the contralateral side when measuring the medial–lateral dimension (depth).⁸ The predicted stabilities according to the Calkins, Keith, and Moed methods, when compared with the results of examinations under anesthesia, were 33.3%, 14.35%,

Table 2: Statistical comparison of three methods for measuring posterior wall fracture fragment percentages

		1	
Patients/methods	Percentages values (mean±SD)	ANOVA (P)	Post hoc analysis (P)
Patient 1			
Axial CT scan	25.9±3.9	0.004	<0.003a
3D reconstruction	38.7±2.4		<0.128b
Gold standard surface area	36.3±2.7		0.602°
Patient 2			
Axial CT scan	56.7±9.2	0.961	
3D reconstruction	59.4±5.7		
Gold standard surface area	59.1±2.3		
Patient 3			
Axial CT scan	46.7±11.3	0.005	0.865^{a}
3D reconstruction	61.1±15.6		0.004^{b}
Gold standard surface area	80.8±5.2		0.101°
Patient 4			
Axial CT scan	69.6±7.6	0.004	0.131a
3D reconstruction	81.2±1.0		0.003^{b}
Gold standard surface area	85.9±4.7		0.608°
Patient 5			
Axial CT scan	36.2±14.7	0.004	0.003a
3D reconstruction	61.7±3.4		0.687^{b}
Gold standard surface area	53.1±1.1		0.120°
Patient 6			
Axial CT scan	21.4±8.6	0.007	0.143a
3D reconstruction	40.1±14.2		0.006^{b}
Gold standard surface area	48.3±3.8		0.772°
Patient 7			
Axial CT scan	25.6±12.1	0.055	
3D reconstruction	40.8±12.6		
Gold standard surface area	35.9±1.9		
Patient 8			
Axial CT scan	67.9±7.2	0.004	0.131a
3D reconstruction	84.5±4.1		0.003^{b}
Gold standard surface area	89.7±4.2		0.607°

⁹Comparison of axial CT scan versus 3D reconstruction; ^bComparison of axial CT scan versus gold standard surface area; ^cComparison of 3D reconstruction versus gold standard surface area. SD=Standard deviation; ANOVA=Analysis of variance; CT=Computed tomography; 3D=3-Dimensional

and 0%, respectively, of the incorrectly predicted rate. These results demonstrate the effect of the measurement method on the predicted rate. However, those authors did not report the inter-and intra-observer reliabilities of their methods. Although Davis and Moed reported that they achieved good intra-observer reliability when using plain radiographs and

Table 3: Intra-class correlation coefficients

Methods	ICC	95% CI for ICC	
Inter-observer reliability			
Axial CT scan	0.950	0.796-0.990	
3D reconstruction	0.949	0.853-0.988	
Gold standard surface area	0.995	0.986-0.999	
Intra-observer reliability (overall)			
Axial CT scan	0.960	.960 0.794-0.992	
3D reconstruction	0.984	0.896-0.997	
Gold standard surface area	0.993	0.967-0.998	
Raters/methods	ICC	95% CI for ICC	
Intra-observer reliability (individual)			
Physician 1			
Axial CT scan	0.949	0.742-0.990	
3D reconstruction	0.982	0.914-0.996	
Gold standard surface area	0.998	0.991-1.000	
Physician 2			
Axial CT scan	0.985	0.931-0.997	
3D reconstruction	0.994	0.971-0.999	
Gold standard surface area	0.987	0.935-0.997	
Physician 3			
Axial CT scan	0.925	0.607-0.985	
3D reconstruction	0.965	0.672-0.994	
Gold standard surface area	0.996	0.974-0.999	
Physician 4			
Axial CT scan	0.992	0.959-0.998	
3D reconstruction	0.991	0.959-0.998	
Gold standard surface area	0.995	0.975-0.999	
Physician 5			
Axial CT scan	0.951	0.735-0.990	
3D reconstruction	0.992	0.964-0.998	
Gold standard surface area	0.991	0.961-0.998	

CT=Computed tomography; 3D=3-Dimensional; ICC=Intra-class correlation coefficient; CI=Confidence interval

axial CT images, the inter-observer reliability was poor.¹³ We determined that a standard and reliable method for measuring the posterior wall fracture fragment percentages was needed because fracture patterns are diverse.

In this study, we established a gold standard method for calculating the total surface area of the intact posterior wall, the surface area of the fracture fragment, and the percentage of the fracture fragment using the Materialise Mimics and 3-matic software programs. The surface area was calculated in a stepwise fashion. Although the surface area of the fracture fragment would represent the numerator in the fracture fragment percentage calculation, no clear measurement criteria

were available for defining the denominator. Accordingly, we defined the posterior acetabular surface as the region surrounded by the three cutting planes and the posterior rim of the acetabulum to eliminate the excess surface area of the ischial spine, although this method may reflect the true surface area of the posterior acetabulum. Unfortunately, this software program is not available at all hospitals, and physicians using this program would require training to familiarize themselves with the use of the software.

The position of the patient during a CT examination could affect the symmetry of the bilateral morphology. Asymmetry of the acetabular morphology in the same axial CT cutting plane could lead to an inaccurate measurement. Our CT scan images were presented with thicknesses of 1-3 mm, and asymmetry in the bilateral morphology led to different results that varied according to the different axial planes selected by each rater. In this study, we developed a new simple method for measuring the fracture fragment percentages on 3D images reconstructed using interpolation software, which transformed the cutting level differences into a linear gradient. Thus, we were able to measure the length of the ideal location on the 3D image without the limitation of the axial images. Using our simple linear calculation method based on 3D reconstruction images, we achieved excellent levels of inter-and intra-observer reliability for each patient in this study, and the results obtained using our new method did not differ significantly from those obtained using the gold standard surface measurement method. We further note that our new method could be performed using the picture archiving and communication system (PACS) and did not require Mimics software. The Mimics and 3-matic software programs enable the direct measurement of actual lengths on the 3D reconstruction images. In PACS, the lengths measured on 3D reconstruction images are based on pixels. We found that the length units obtained using PACSs did not affect the fracture fragment percentage. Therefore, our new method could replace the traditional axial CT scan method as a preoperative assessment tool.

Although we achieved excellent inter-and intra-observer reliabilities with the axial CT scan method, the true percentages differed significantly from those determined using the gold standard method in four (50%) patients and three had fracture fragments exceeding 80%. One patient (patient 6) had a comminuted posterior wall fracture fragment located near the posterior column, and the rater found it difficult to select the appropriate axial CT scan cut. Furthermore, when the comminuted posterior wall fragment was located near the acetabular rim, the axial CT and gold standard surface area method measurements did not differ significantly. We concluded that the axial CT scan method could not be used

accurately in patients with larger (>80%) fragments or with comminution near the posterior column region.

Simultaneous open reduction and internal fixation and acute total hip replacement (THR) or primary THR are available treatment options for elderly patients after displaced acetabular fractures. 14-17 The percentage of posterior wall fragments may affect the bony coverage of the acetabular cup. Potentially, our new measurement method could be used for the preoperative evaluation of such cases. Our method may also be useful for measuring the acetabular posterior wall defect percentage in cases of revision total hip arthroplasty.

This study had several limitations of note. First, we only measured the posterior wall fracture fragment percentage and did not compare the correlation between hip stability and the fragment percentage measured by the new method. This will be addressed in a further study. We note that as the true surface area of the acetabulum and fracture fragment measurements depend on the imaging software, raters should be trained thoroughly to ensure accurate calculations. Second, the number of patients was relatively small because we focused only on cases of simple posterior wall fractures, which were reviewed by only five raters. Despite these limitations, all the raters were asked to perform all measurements twice to reduce the bias encountered in the study setting.

CONCLUSION

We established a standard posterior acetabular surface area and fracture fragment surface area measurement technique using 3D reconstruction image software. We also developed a new and simple method for calculating the posterior wall fracture fragment percentage using 3D reconstruction image data. We achieved excellent inter-and intra-observer reliabilities with this new method. Pelvis fracture is critical for trauma patients, and we could rely on this method to provide personalized operation for a wide variety of pelvic fractures.

Data availability statement

The data that support the findings of this study are available from the corresponding author, Yeh TT, upon reasonable request.

Financial support and sponsorship

This work was supported by the Tri-Service General Hospital (TSGH-D-110105, TSGH-B-110008, MND-MAB-110-016, TSGH-NTUST-109-04, TSGH-A-109004, TSGH-B-109007, TSGH-C108-001, MAB-108-034, TSGH-C107-001, TSGH-B-111015 and MND-MAB-111035).

Conflicts of interest

There are no conflicts of interest.

REFERENCES

- Hsu CL, Chou YC, Li YT, Chen JE, Hung CC, Wu CC, et al. Pre-operative virtual simulation and three-dimensional printing techniques for the surgical management of acetabular fractures. Int Orthop 2019;43:1969-76.
- Firoozabadi R, Hamilton B, Toogood P, Routt MC, Shearer D. Risk factors for conversion to total hip arthroplasty after acetabular fractures involving the posterior wall. J Orthop Trauma 2018;32:607-11.
- 3. Klasan A, Neri T, Sommer C, Leie MA, Dworschak P, Schofer MD, *et al.* Analysis of acetabular version: Retroversion prevalence, age, side and gender correlations. J Orthop Translat 2019;18:7-12.
- 4. Harnroongroj T, Riansuwan K, Sudjai N, Harnroongroj T. Posterior acetabular arc angle of unstable posterior hip fracture-dislocation. Int Orthop 2013;37:2443-9.
- Harnroongroj T, Suangyanon P, Tharmviboonsri T, Harnroongroj T. Posterior acetabular arc angle of the femoral head assesses instability of posterior fracture-dislocation of the hip. Int Orthop 2013;37:1141-5.
- 6. Liu Q, Cheng X, Yan D, Zhou Y. Plain radiography findings to predict dislocation after total hip arthroplasty. J Orthop Translat 2019;18:1-6.
- 7. Reagan JM, Moed BR. Can computed tomography predict hip stability in posterior wall acetabular fractures? Clin Orthop Relat Res 2011;469:2035-41.
- 8. Moed BR, Ajibade DA, Israel H. Computed tomography as a predictor of hip stability status in posterior wall fractures of the acetabulum. J Orthop Trauma 2009;23:7-15.
- 9. Koo TK, Li MY. A guideline of selecting and reporting intraclass correlation coefficients for reliability research. J Chiropr Med 2016;15:155-63.
- Portney L.G., Watkins M.P. Foundations of Clinical Research: Applications to Practice. 3rd ed. Pearson Prentice Hall; Upper Saddle River, NJ, USA: 2009.
- 11. Firoozabadi R, Spitler C, Schlepp C, Hamilton B, Agel J, Routt MC, *et al.* Determining stability in posterior wall acetabular fractures. J Orthop Trauma 2015;29:465-9.
- 12. Hettich G, Schierjott RA, Ramm H, Graichen H, Jansson V, Rudert M, *et al.* Method for quantitative assessment of acetabular bone defects. J Orthop Res 2019;37:181-9.
- 13. Davis AT, Moed BR. Can experts in acetabular fracture care determine hip stability after posterior wall fractures using plain radiographs and computed tomography? J Orthop Trauma 2013;27:587-91.
- 14. Giunta JC, Tronc C, Kerschbaumer G, Milaire M, Ruatti S, Tonetti J, *et al.* Outcomes of acetabular fractures in the elderly: A five year retrospective study of twenty

- seven patients with primary total hip replacement. Int Orthop 2019;43:2383-9.
- 15. Makridis KG, Obakponovwe O, Bobak P, Giannoudis PV. Total hip arthroplasty after acetabular fracture: Incidence of complications, reoperation rates and functional outcomes: evidence today. J Arthroplasty 2014;29:1983-90.
- 16. Malhotra R, Singh DP, Jain V, Kumar V, Singh R. Acute
- total hip arthroplasty in acetabular fractures in the elderly using the octopus system: Midterm to long term follow-up. J Arthroplasty 2013;28:1005-9.
- 17. Salama W, Mousa S, Khalefa A, Sleem A, Kenawey M, Ravera L, *et al.* Simultaneous open reduction and internal fixation and total hip arthroplasty for the treatment of osteoporotic acetabular fractures. Int Orthop 2017;41:181-9.